ROLES OF PARTICLE LENGTH AND DEGREE OF POLYMERIZATION IN THE DISSOLUTION OF BAMBOO-DERIVED CELLULOSE IN LOW-TEMPERATURE AQUEOUS NaOH

TARO KINUMOTO,[*,**] YUKA TANOUE,[***] KAZUKI NAMBA,[***] XINYU LI,[***] MIKI MATSUOKA[*] and MASAYA MORIYAMA[*]

[*]*Applied Chemistry Cluster, Faculty of Science and Technology, Oita University 700 Dannoharu, Oita, 870-1192, Japan*
[**]*Research Center for Advanced Technology and GX, Oita University, 700 Dannoharu, Oita, 870-1192, Japan*
[***]*Applied Chemistry Course, Graduate School of Engineering, Oita University, 700 Dannoharu, Oita, 870-1192, Japan*
✉ *Corresponding authors: T. Kinumoto, kinumoto@oita-u.ac.jp*
M. Moriyama, morimasa@oita-u.ac.jp

Received June 15, 2026

The dissolution behavior of bamboo-derived cellulose (BC) was investigated in a two-step low-temperature aqueous NaOH system using commercial cellulose (CC) as a reference. The study focused on feedstock-related factors, particularly particle length and viscosity-average degree of polymerization (*DPv*). Characterization of the feedstock powders showed that BC differed from CC in having a longer particle length and a higher *DPv*.
During dissolution in aqueous NaOH, both BC and CC underwent swelling and mercerization; however, complete dissolution was not achieved under the conditions examined in this study. BC consistently showed lower solubility than CC, and this difference was discussed in relation to its particle length and *DPv*, with possible contributions from solvent accessibility. The *DPv* values of the cellulose recovered from the aqueous NaOH solution converged to approximately 180, suggesting an apparent *DPv* limitation under the present dissolution conditions. Particle-length fractionation of BC increased the proportion of shorter particles, decreased *DPv*, and improved solubility, indicating that feedstock fractionation is a practical approach for improving BC dissolution in aqueous NaOH.
As a proof-of-concept recovery experiment, alkali-dissolved cellulose fractions were treated using aqueous acetic acid, yielding cellulose II-containing solid products. These findings provide useful guidance for processing bamboo-derived cellulose powders in low-temperature aqueous NaOH and for developing simple recovery routes for cellulose products from bamboo resources.

Keywords: bamboo-derived cellulose, aqueous NaOH dissolution, particle-length fractionation, viscosity-average degree of polymerization, cellulose recovery

INTRODUCTION

Cellulose is the most abundant natural polymer and is widely used in materials such as pulp, paper, fibers, films, and cellulose-based composites. Because native cellulose has a highly ordered structure stabilized by intra- and intermolecular hydrogen bonding, its dissolution is an important but challenging step in the processing of cellulose-based materials. The efficiency of cellulose dissolution depends not only on the solvent system, but also on the structural characteristics of the cellulose feedstock, including degree of polymerization, crystallinity, morphology, and solvent accessibility.

Among the various solvent systems developed for cellulose processing, low-temperature aqueous sodium hydroxide (NaOH) systems, with or without additives such as urea or thiourea, have been widely studied due to their simple composition and relatively low environmental impact.[1-6] However, cellulose dissolution in aqueous NaOH is sensitive to both solvent conditions and feedstock characteristics, such as

the degree of polymerization and supramolecular structure of cellulose, including crystallinity and solvent accessibility.[1-3] For example, cellulose dissolution in aqueous NaOH without additives is generally limited to a narrow NaOH concentration range of approximately 7-10 wt% at temperatures below 1 °C.[6] Even under these conditions, complete dissolution is not always achieved, highlighting the importance of both solvent conditions and feedstock characteristics in determining cellulose solubility.

Bamboo is a typical and abundant lignocellulosic biomass resource that grows rapidly and is widely available in many regions. Mature bamboo culms consist mainly of cellulose, together with hemicelluloses and lignin, and bamboo-derived cellulose has been investigated for use in materials such as pulp, fibers, and cellulose nanomaterials.[7-10] Depending on the source and preparation process, bamboo-derived cellulose powders may exhibit distinct feedstock characteristics, including particle morphology and degree of polymerization. However, the relationship between these characteristics and dissolution behavior in low-temperature aqueous NaOH remains unclear for bamboo-derived cellulose powders.

In this study, the dissolution behavior of cellulose purified from naturally grown moso bamboo (*Phyllostachys edulis*) was investigated in a two-step low-temperature aqueous NaOH system, using commercial cellulose as a reference. The study focused on the roles of particle length and viscosity-average degree of polymerization (*DPv*) in the dissolution behavior of bamboo-derived cellulose. The particle morphology, *DPv*, crystalline characteristics, and solubility of BC and CC were compared, and the effect of particle-length fractionation on BC dissolution was examined. The *DPv* of the recovered cellulose fraction was also evaluated to discuss the apparent *DPv* limitation under the present conditions. Aqueous acetic acid was further used for proof-of-concept recovery of cellulose from the alkali-dissolved fraction. This study provides practical insights into feedstock-related factors affecting the aqueous NaOH processing of bamboo-derived cellulose powders.

EXPERIMENTAL

Materials

Chemically bleached bamboo-derived cellulose (BC) powder prepared from moso bamboo (*Phyllostachys edulis*) was supplied by Oita CELEENA Co., Ltd. The BC powder was used without high-intensity mechanical pretreatment to examine the dissolution behavior of the as-received bamboo-derived cellulose powder. Commercial cellulose (CC) powder was purchased from FUJIFILM Wako Pure Chemical Co. (Product No. 034-22221) and used as a reference material. According to the supplier, the CC powder was specified to pass through a 38 μm mesh. To match the particle size distribution of CC, the BC powder was sieved for 15 min using an electric sieve shaker equipped with a 38 μm-aperture sieve to remove coarse particles and agglomerates. Aqueous NaOH solutions were prepared from 10 mol dm^{-3} (M) NaOH solution (Kishida Chemical Co., Ltd., 900-02185). Acetic acid (FUJIFILM Wako Pure Chemical Co., 014-00261) was used to prepare the aqueous coagulation bath for cellulose recovery. Cupriethylenediamine hydroxide solution ($Cu(H_2NCH_2CH_2NH_2)_2(OH)_2$, CED solution; GFS Chemicals, 32103 1L) was used for determining the viscosity-average degree of polymerization (*DPv*). Ultrapure water with a resistivity of ≥ 18.2 MΩ cm was used throughout the study.

Characterization of BC and CC powders

The particle morphology of BC and CC powders was observed using a digital microscope (Keyence, VHX-500F) at 250× magnification. Because both samples contained elongated particles with aspect ratios greater than unity, the minor and major axes of each particle were defined as the particle diameter and particle length, respectively. For each sample, 300 randomly selected particles were measured to obtain the particle-size distributions.

Fourier-transform infrared (FT-IR) spectra were recorded using an IR spectrometer (Thermo Fisher Scientific, Nicolet iS5) equipped with an attenuated total reflection accessory (iD5 ATR). Spectra were collected over the wavenumber range of 4000–550 cm^{-1}. X-ray diffraction (XRD) measurements were performed using an X-ray diffractometer (Rigaku Corporation, MiniFlex 600) with Cu Kα radiation. Each powder sample was packed into a standard sample holder, leveled with a glass slide, and scanned over a 2θ range of 10-80° at a scanning speed of 10° min^{-1} with a step size of 0.05°.

The *DPv* of each cellulose powder was determined by a viscometric method based on the Japanese Pharmacopoeia using CED solution.[11] Each cellulose sample was dissolved in 0.5 M CED solution under nitrogen bubbling, and the solution was shaken at room temperature for 2 h. A reference solution was prepared in the same manner without cellulose.

Kinematic viscosity measurements were conducted using Ubbelohde viscometers (SIBATA Scientific Technology) at 25.0 ± 0.1 °C. Measurements were performed using three independently prepared solutions. For each solution, the efflux time was measured ten times, and the average value was used for calculation.

The kinematic viscosity, v, was calculated using Equation (1):

$$v = K \times t \quad (1)$$

where K is the viscometer constant and t is the efflux time. The relative viscosity, η_{rel}, was calculated using Equation (2):

$$\eta_{rel} = v_{test} / v_{ref} \quad (2)$$

where v_{test} and v_{ref} are the kinematic viscosities of the cellulose solution and reference solution, respectively. The intrinsic viscosity, $[\eta]C$, was obtained according to the Japanese Pharmacopoeia procedure,[11] and DPv was calculated using Equation (3):

$$DPv = 95\ [\eta]C / M_{cell} \quad (3)$$

where M_{cell} is the mass of cellulose used for preparing the test solution. The same procedure was applied to the recovered cellulose samples to evaluate the DPv of the cellulose fraction recovered from the alkali-dissolved solution.

The cellulose, hemicelluloses, and lignin contents of BC and CC were determined by Tokai Techno Co., Ltd. using the detergent analysis method based on the Van Soest procedure, as described in literature.[12]

Low-temperature aqueous NaOH dissolution

Dissolution experiments were conducted using a two-step low-temperature aqueous NaOH procedure based on the method reported by Yamane *et al*.[2] The procedure is summarized in Figure 1.

In Step I, each cellulose sample was added to a 1.39 M aqueous NaOH solution at a cellulose loading of 3 or 5 wt%. The 3 wt% loading was selected by referring to cellulose concentrations used in previous studies of low-temperature aqueous alkali dissolution systems, whereas the 5 wt% loading was used to examine dissolution behavior at a higher cellulose loading. The suspension was homogenized at 12,000 rpm for 2 min and then cooled to −2 °C.

In Step II, a pre-cooled 5.28 M aqueous NaOH solution was added to obtain a final NaOH concentration of 2.14 M, corresponding to 7.6 wt%. The mixture was homogenized again at 12,000 rpm for 2 min under cooling. This two-step procedure was selected based on preliminary trials, in which direct preparation at the final NaOH concentration resulted in lower cellulose solubility under the present conditions.

In Step III, the mixture was centrifuged at 5 °C and 20,000 rpm for 1 h. The supernatant was collected as the alkali-dissolved cellulose solution. Because complete dissolution was not achieved under the conditions examined in this study, this centrifugation step was used to separate the insoluble residue from the dissolved cellulose fraction.

The dissolution state was evaluated by visual observation, transmittance measurement, and optical microscopy. Transmittance, including diffusely transmitted light, was measured at 660 nm using a UV-Vis spectrophotometer (Jasco Corporation, V-650) equipped with an integrating sphere (Jasco Corporation, ISV-922).

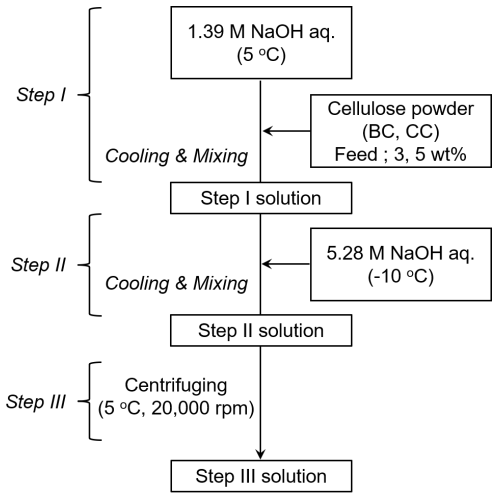


Figure 1: Flowchart for cellulose dissolution procedure

Determination of cellulose solubility

Cellulose solubility was determined from the amount of cellulose recovered from the supernatant after centrifugation. A 1.0 M HCl solution was added to the supernatant to precipitate the dissolved cellulose. The precipitate was collected by vacuum filtration using a pre-weighed PTFE membrane filter (Advantec, H010A047A), washed with ultrapure water, and dried at 60 °C for at least 12 h.

The solubility was calculated as the mass of dried cellulose recovered from the supernatant divided by the initial mass of cellulose added to the NaOH solution. Therefore, the solubility value in this study represents the fraction of cellulose that was transferred to the centrifuged supernatant and recovered by acid precipitation. All dissolution experiments were performed in triplicate, and the results are reported as the mean and standard deviation.

Particle-length fractionation of BC

To examine the effect of particle length on BC dissolution, part of the BC powder sieved through the 38 μm-aperture sieve was further fractionated using a 20 μm-aperture sieve. The original and further fractionated BC samples are referred to as BC38 and BC20, respectively. The particle morphology, *DPv*, and solubility of BC20 were evaluated using the same procedures described above.

Recovery of cellulose using aqueous acetic acid

As a proof-of-concept experiment, cellulose recovery was examined by extruding the alkali-dissolved cellulose solution into an aqueous acetic acid solution. The cellulose solution obtained after Step III was extruded into 1 L of 2.5 M aqueous acetic acid using a syringe equipped with a 0.6 mm-diameter needle. The recovered specimens were kept in the acetic acid solution for 2 min, washed by immersion in ultrapure water for 5 min, and then dried at 60 °C.

The cellulose specimens recovered from BC and CC are hereafter referred to as RBC and RCC, respectively. FT-IR, XRD, and *DPv* measurements were performed on the recovered specimens. Their morphology was observed by scanning electron microscopy (SEM; Hitachi High-Technologies, Miniscope TM3000), and their optical anisotropy was examined by polarized optical microscopy (Olympus, BX51) under "crossed Nicols".

RESULTS AND DISCUSSION

Feedstock characteristics of BC and CC

The results of the particle morphology analysis of BC and CC conducted using digital microscopy are presented in Figure 2. Here, the mean width was determined based on the statistical resolution of the optical microscopy measurements. The key statistical data (mean, standard deviation, and median) are summarized in Table 1. The diameter distributions for BC and CC (Fig. 2a and 2b) were similar, and the comparable mean and median values confirmed that the particle diameters of BC and CC were essentially identical. By contrast, the particle lengths of BC and CC differed significantly. The length distribution of BC (Fig. 2c) is clearly shifted toward larger values relative to that of CC (Fig. 2d), with the median length of BC longer than that of CC by approximately 25 μm. The *DPv* values are also listed in Table 1, which shows that the *DPv* of BC (approximately 360) was substantially higher than that of CC (approximately 260).

The viscosity-averaged molecular weight (*Mv*) was calculated using Equation (4), yielding 5.9×10^4 and 4.2×10^4 for BC and CC, respectively. Here, 162.14 is the molecular weight of the anhydroglucose unit.

$$Mv = DPv \times 162.14 \quad (4)$$

To assess the validity of the *DPv* and *Mv* values for BC, the number-average (*Mn*) and weight-average (*Mw*) molecular weights were measured by gel permeation chromatography. The values were determined using a pullulan (Shodex, STANDARD P-82) calibration curve and expressed as pullulan-equivalent values.

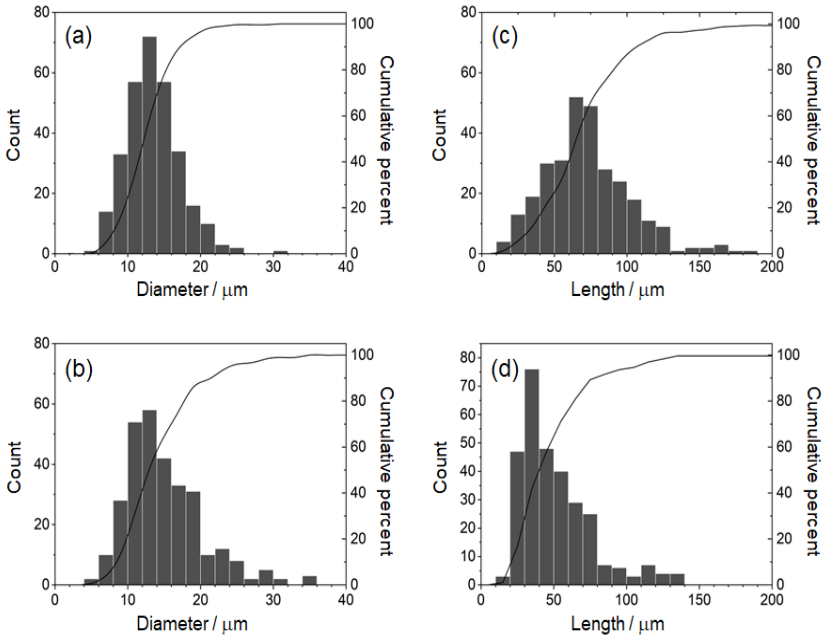


Figure 2: Distribution of diameter (a and b) and length (c and d) for BC (a and c) and CC (b and d).

Table 1
Particle size, *DPv*, crystallinity index and chemical composition of bamboo-derived cellulose (BC) and commercial cellulose (CC)

	Diameter (μm)			Length (μm)			*DPv*	CI	Content (%)		
	Avg.	*SD*	*Med.*	*Avg.*	*SD*	*Med.*		(%)	*Cel.*	*Hem.*	*Lig.*
BC	14	4	13	74	33	70	360	ca. 55	96	4	0
CC	15	5	14	52	26	45	260	ca. 80	94	6	0

Particle diameter and length are expressed as average (*Avg.*), standard deviation (*SD*), and median (*Med.*) values; *Cel.*, *Hem.*, and *Lig.* denote cellulose, hemicelluloses, and lignin, respectively

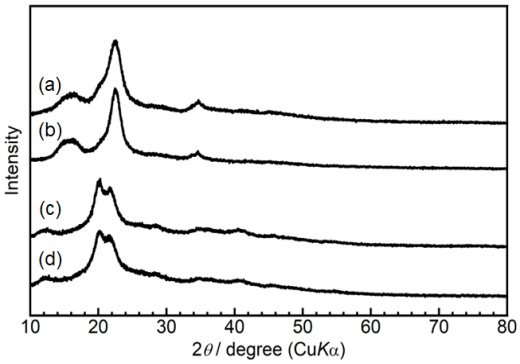


Figure 3: XRD patterns of (a) BC, (b) CC, (c) RBC and (d) RCC

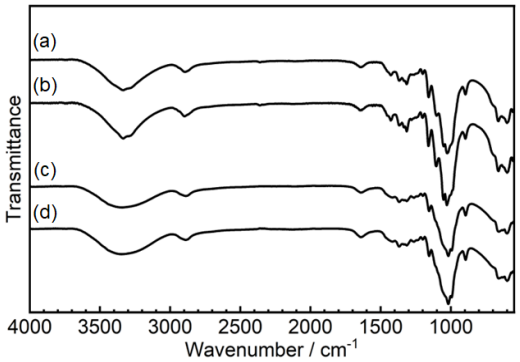


Figure 4: FT-IR spectra of (a) BC, (b) CC, (c) RBC and (d) RCC

The measured *Mn* and *Mw* of BC were 1.2×10^4 and 1.0×10^5, respectively. *Mv* lies between *Mn* and *Mw*, clearly demonstrating the validity of the *DPv* values. The difference of approximately 100 between the *DPv* values of BC and CC corresponds to the *Mv* difference of approximately 1.7×10^4.

The clear differences in the particle length and degree of polymerization between BC and CC were expected to significantly affect their solubility in aqueous NaOH solutions. Isogai *et al.* reported that the solubility of cellulose in aqueous NaOH solutions is correlated with the degree of long-range order disruption,[3] which in turn has been reported to be correlated with specific alkaline conditions. However, the degree of long-range order disruption cannot be quantified directly. Therefore, to gain indirect insights into long-range order and its influence on dissolution, we examined the crystallinity of BC and CC using XRD measurements. The obtained XRD patterns are shown in Figure 3. As shown in Figures 3a and 3b, both BC and CC exhibit diffraction peaks characteristic of cellulose I, with the overlapping (110)/(110B) reflections observed at $2\theta \approx 15°$ and the (200) reflection at $2\theta \approx 22.5°$.

The crystallinity index (CI) was calculated using Equation 5, as proposed by Isogai and Usuda.[13] In this method, the diffraction intensity of the (110) reflection (I_{110}) and amorphous contribution at the same diffraction angle (I_{110B}) were used. For cellulose I, a correction factor (a = 1.25) was applied to adjust the CI values to be comparable to those obtained using the conventional Segal method.

$$CI\ (\%) = a \times (I_{1\bar{1}0} - I_{1\bar{1}0B}) / I_{1\bar{1}0} \quad (5)$$

As summarized in Table 1, BC exhibited a lower CI than CC. Together with the results for particle size and degree of polymerization, the XRD results show that BC is characterized by a diameter comparable to that of CC, but exhibits longer length and lower crystallinity.

The FT-IR spectra of BC and CC are shown in Figure 4a and 4b, respectively. Both spectra showed characteristic absorption bands of cellulose, and no clearly assignable peaks attributable to lignin or hemicelluloses were observed. As summarized in Table 1, chemical composition analysis showed that the cellulose contents of BC and CC were 96% and 94%, respectively, indicating that both samples consisted predominantly of cellulose. The hemicellulose contents were 4% for BC and 6% for CC, while the lignin contents were reported as 0% for both samples. These results indicate that BC and CC had similar chemical compositions, with only minor differences in their cellulose and hemicellulose contents.

In addition, thermogravimetric analysis (Rigaku Corporation, TG-DTA8122) conducted in air up to 1000 °C showed no discernible residual mass for either sample, suggesting that their ash contents were very low. These results indicate that BC and CC had similar chemical compositions, with only minor differences in their cellulose and hemicellulose contents. Isogai and Atalla reported that the presence of hemicelluloses does not necessarily prevent cellulose dissolution in aqueous NaOH, because most hemicellulose fractions are soluble under alkaline conditions.[3] In addition, Xu *et al.* treated bamboo pulp containing approximately 15% hemicelluloses with NaOH/urea and subsequently reported its dissolution in a NaOH/ZnO solution.[14] Notably, the FT-IR spectrum of their bamboo-derived pulp exhibited a characteristic xylan-related C=O band at 1640 cm^{-1}, which was absent from the BC spectrum obtained in the present study. Therefore, for the purpose of discussing cellulose dissolution behavior, BC can be regarded as a sufficiently purified cellulose powder, and the residual hemicelluloses in BC can be reasonably neglected as a dominant factor in this aqueous NaOH system. Accordingly, the following discussion focuses mainly on particle morphology, *DPv*, and crystalline characteristics as feedstock-related parameters affecting dissolution behavior.

Dissolution behavior of BC and CC in low-temperature aqueous NaOH

The appearance of the BC and CC mixtures, the transmittance including diffusely transmitted light, and the optical micrographs obtained during the dissolution procedure are shown in Figures 5, 6, and 7, respectively.

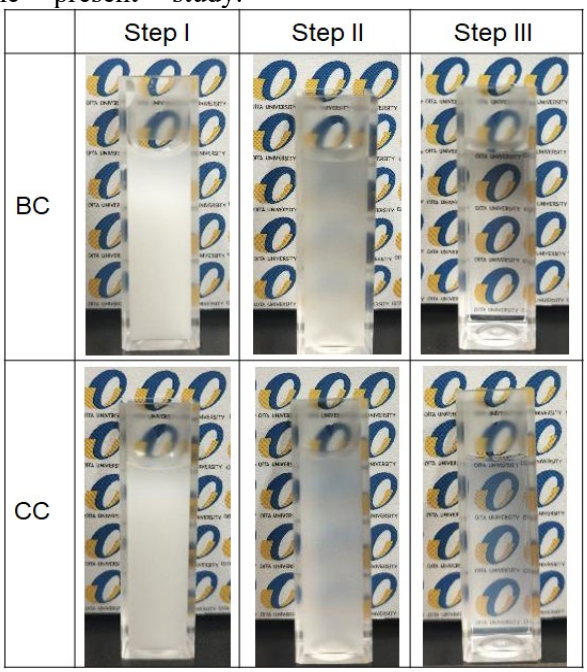


Figure 5: Changes in the turbidity of the solutions at each step at feed ratio = 3%

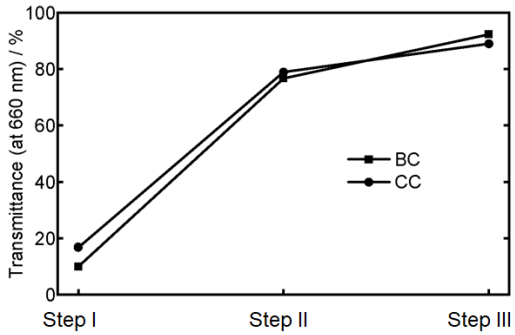


Figure 6: Transmittance including diffusely transmitted light at 660 nm of the solution at each step at feed ratio = 3%

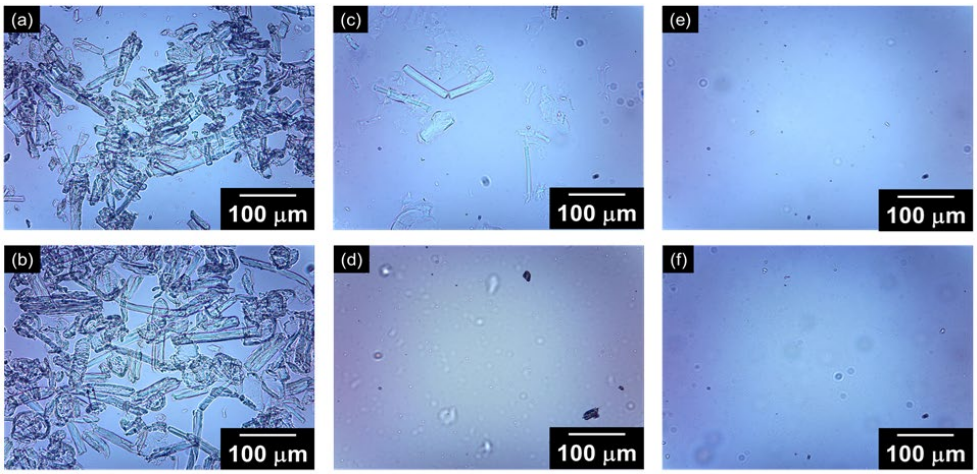


Figure 7: Optical microscopy images of the cellulose solutions at each step at feed ratio = 3%: (a) BC at step I, (b) CC at step I, (c) BC at step II, (d) CC at step II, (e) BC at step III, and (f) CC at step III

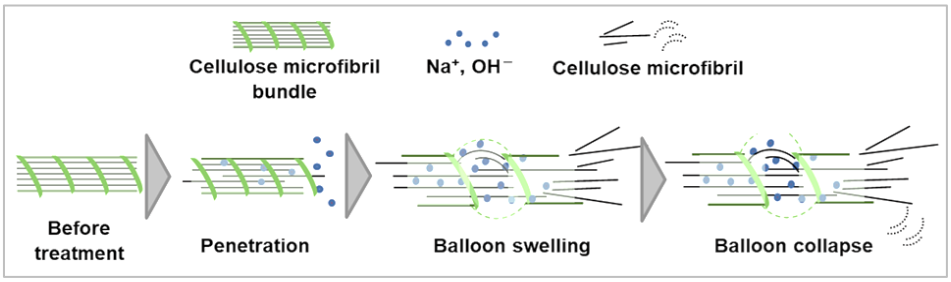


Figure 8: Schematic of mercerization

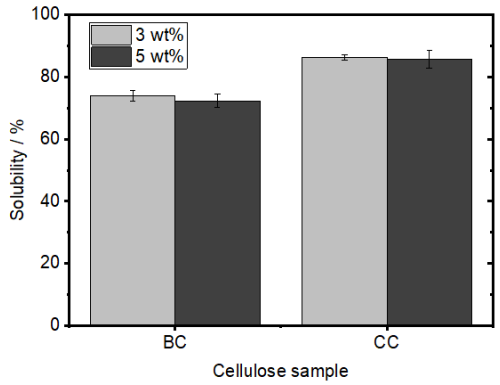


Figure 9: Comparison of cellulose solubility of BC and CC at cellulose loadings of 3 and 5 wt% (columns represent the mean values, and error bars represent the standard deviations of three independent measurements)

The results shown here were obtained at a feed ratio of 3 wt%. After Step I, both mixtures were turbid, and their transmittance values were below 20%. Optical microscopy confirmed the presence of many cellulose particles, indicating that a large fraction of the cellulose remained undissolved at this stage. After Step II, the turbidity of both mixtures decreased markedly, and the transmittance increased to approximately 80%. Optical microscopy showed swelling of the cellulose particles after Step II, with balloon-like morphologies being particularly evident for BC, as shown in Figure 7c. This behavior is consistent with mercerization (Fig. 8), in which aqueous NaOH penetrates into cellulose particles and promotes swelling through the disruption and rearrangement of hydrogen-bonding networks. The swelling appeared more prominent for BC than for CC, probably because the longer BC particles made the deformation easier to observe under the same magnification.

After centrifugation in Step III, transparent supernatants were obtained for both BC and CC. The increase in transmittance and the absence of

clearly visible cellulose particles in the optical micrographs (Fig. 7e and 7f) indicate that the insoluble residues were effectively removed by centrifugation. Thus, the supernatant obtained after Step III was treated as the alkali-dissolved cellulose fraction in this study.

The cellulose solubility, calculated from the amount of HCl-precipitated cellulose recovered from the supernatant, is shown in Figure 9 for two representative cellulose loadings, 3 and 5 wt%. Under these conditions, complete dissolution was not achieved for either BC or CC, indicating that part of the added cellulose remained as an insoluble fraction. At both loadings, CC showed higher solubility than BC, suggesting that BC was less readily dissolved under the present low-temperature aqueous NaOH conditions.

The lower solubility of BC can be discussed in relation to the feedstock characteristics described above. BC had a longer particle length and higher *DPv* than CC, while both samples showed cellulose I characteristics. Longer particles may require longer diffusion pathways for water molecules and hydroxide ions to penetrate into the particle interior, which could retard swelling and mercerization. A higher *DPv* may also contribute to lower solubility by reducing the fraction of cellulose chains that can dissolve in aqueous NaOH under the present conditions. Although the individual contributions of particle morphology, *DPv*, crystallinity, and solvent accessibility cannot be separated from the present data, these feedstock-related parameters should be considered when discussing the lower solubility of BC. This point is further examined through the *DPv* of the recovered cellulose fraction and particle-length fractionation in the following sections.

Apparent *DPv* limitation of the recovered fraction

The alkali-dissolved fractions of BC and CC were precipitated using aqueous acetic acid, and the recovered products are hereafter referred to as RBC and RCC, respectively. As summarized in Table 2, both RBC and RCC showed *DPv* values of approximately 180, despite the different initial *DPv* values of BC and CC.

This convergence is comparable to the leveling-off DP reported for cellulose dissolution in low-temperature aqueous NaOH systems by Isogai and Atalla,[3] although their procedure involved a freeze-thaw treatment that was not used in the present study. Therefore, the *DPv* value of approximately 180 observed here is considered to reflect an apparent *DPv* limitation of the recovered cellulose fraction under the present dissolution and recovery conditions.

It should be noted that this result does not by itself prove selective dissolution of low-*DPv* cellulose fractions, because the *DPv* and structure of the undissolved residues were not examined in this study. In addition, a partial contribution from chain scission during dissolution or in the dissolved state cannot be completely excluded. Previous studies have reported decreases in the molecular weight of cellulose in NaOH-based systems during storage or under intensive mechanical treatment, depending on the processing conditions.[15,16] In the present system, the dissolution process was conducted at low temperature for a short duration and without oxidative reagents; therefore, extensive alkaline degradation is unlikely to be the sole explanation for the observed *DPv* decrease. Nevertheless, the *DPv* convergence should be interpreted cautiously as an apparent limitation of the recovered fraction rather than as direct evidence of selective dissolution.

Overall, the *DPv* results indicate that the cellulose fraction recovered from the alkali-dissolved solution had a lower and similar *DPv*, regardless of the starting cellulose source. This finding provides a useful constraint for discussing the cellulose fraction that was transferred into the alkali-dissolved solution and recovered under the present conditions, without relying on a definitive assignment of the molecular-weight distribution of the undissolved fraction.

Table 2
DPv of RBC and RCC

Sample	*DPv*
RBC	188
RCC	183

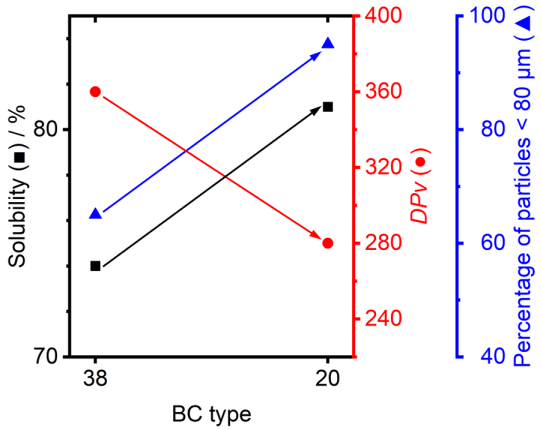


Figure 10: Solubility, *DP*v, and percentage of particles smaller than 80 µm for BC38 and BC20

Effect of particle-length fractionation on BC dissolution

The results described above suggest that the lower solubility of BC may be related, at least in part, to its longer particle length and higher *DPv*. To further examine the effect of particle-length reduction on BC dissolution, a portion of the BC powder sieved through a 38 µm-aperture sieve was further fractionated using a 20 µm-aperture sieve. The original and further fractionated BC samples are referred to as BC38 and BC20, respectively.

The particle-length distributions and *DPv* values of BC38 and BC20 are shown in Figure 10. The additional sieving step reduced the particle length of BC and increased the fraction of shorter particles. The proportion of particles shorter than 80 µm increased to approximately 95%, and the *DPv* decreased to approximately 280. These results indicate that the fractionation changed both the particle morphology and the average degree of polymerization of the BC powder.

BC20 showed higher solubility than BC38 under the same aqueous NaOH dissolution conditions. This improvement suggests that particle-length fractionation is an effective practical approach for increasing the amount of BC transferred into the alkali-dissolved fraction. The shorter particle length may reduce the diffusion distance required for water molecules and hydroxide ions to penetrate into the particle interior, thereby facilitating swelling and mercerization.

This improvement was accompanied by both a reduced *DPv* and an increased fraction of short particles, suggesting that particle length and *DPv* are relevant feedstock-related parameters for improving BC dissolution under the present aqueous NaOH conditions.

Recovery of cellulose using aqueous acetic acid

As a proof-of-concept experiment, recovery of fibrous cellulose products from the alkali-dissolved fraction was examined using aqueous acetic acid. Cellulose dissolved in alkaline solution is expected to precipitate when the solution is neutralized or acidified, owing to the reformation of hydrogen-bonding networks. In preliminary tests, sulfuric acid led to the incorporation of sulfur-containing impurities into the recovered products, whereas acetic acid did not introduce detectable inorganic impurities. Therefore, 2.5 M aqueous acetic acid was selected as the recovery bath in this study.

The appearance of fibrous RBC and RCC is shown in Figure 11. Extrusion of the alkali-dissolved solutions into the acetic acid bath yielded fibrous regenerated cellulose specimens. These specimens were brittle under the present non-optimized conditions and fractured during handling for tensile testing; therefore, this experiment is regarded as proof-of-concept cellulose recovery rather than optimized fiber production.

SEM images of RBC and RCC are shown in Figure 12. The cut cross-sections contained both relatively flat regions and porous regions with small void-like features. Because the cross-sections were prepared by mechanical cutting, these local features should be interpreted as morphological observations of the fractured/cut surface rather than as evidence of a uniformly dense internal structure. The side surfaces also showed surface irregularities and discontinuous features, indicating structural heterogeneity of the regenerated specimens.

The XRD patterns of the recovered samples are shown in Figures 3c and 3d. The diffraction profiles differed from those of the original cellulose powders shown in Figures 3a and 3b. The characteristic cellulose I reflections in the $2\theta \approx 14$-$16°$ region became less apparent after recovery, whereas a low-angle reflection at approximately $2\theta \approx 12°$ and a broad diffraction feature in the $2\theta \approx 20$-$22°$ region were observed. These changes are consistent with the formation of cellulose II during dissolution and regeneration.

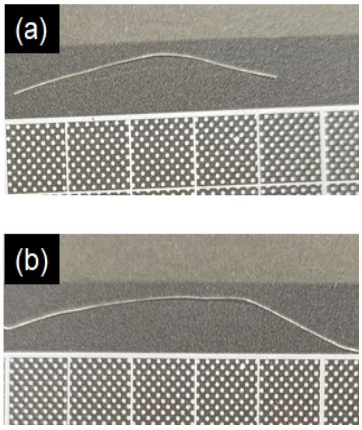


Figure 11: Appearance of (a) RBC and (b) RCC

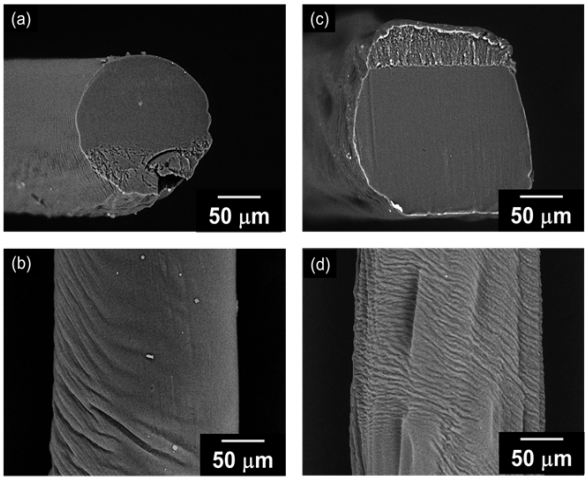


Figure 12: Representative SEM images of RBC (a, b) and RCC (c, d); cross-sectional (a, c) and side (b, d) views

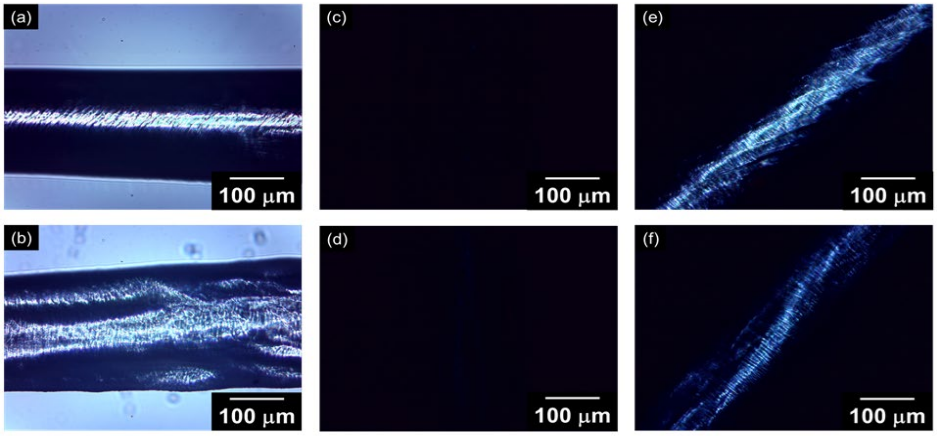


Figure 13: Optical microscopic images of RBC (a, c, e) and RCC (b, d, f) fibers; Non-polarized (a, b) and polarized observations under crossed Nicols (c, d) of fibers placed horizontally (extinction position); Polarized optical microscopic images observed under crossed Nicols (e, f) of fibers placed at 45° (diagonal position)

The FT-IR spectra of RBC and RCC are shown in Figure 4c and 4d, respectively. Compared with the original BC and CC powders, the O-H stretching region became broader after recovery. The band at approximately 1430 cm^{-1}, which is often associated with CH_2 bending and is sensitive to the cellulose I crystalline structure, was attenuated. In addition, the characteristic cellulose I-related absorption near 1100 cm^{-1} was no longer clearly resolved in the recovered specimens. These spectral changes are consistent with the structural transition from cellulose I to cellulose II, in agreement with the XRD results.

POM observations were performed to examine the optical anisotropy of the recovered specimens. Under crossed Nicols, RBC and RCC showed angle-dependent changes in brightness: the specimens appeared dark near the extinction position and brighter when placed at approximately 45° to the polarizer/analyzer direction, as shown in Figure 13. This angle-dependent birefringence indicates optical anisotropy of the recovered specimens and is consistent with partial alignment of cellulose domains during extrusion and recovery. However, quantitative orientation analysis was not performed in this study; therefore, the POM results should not be interpreted as direct evidence of a highly oriented cellulose structure.

Overall, these results indicate that the alkali-dissolved cellulose fraction obtained from BC and CC can be recovered as cellulose II-containing solid products using aqueous acetic acid. The recovered specimens were brittle and structurally heterogeneous under the present conditions, indicating that the recovery process was not optimized for mechanical performance. Nevertheless, the results demonstrate the feasibility of proof-of-concept cellulose recovery from bamboo-derived cellulose using a simple NaOH dissolution–acetic acid recovery process.

CONCLUSION

The dissolution and recovery behavior of BC in a two-step low-temperature aqueous NaOH system was investigated using CC as a reference. BC was characterized by a longer particle length and higher *DPv* than CC, while both samples exhibited cellulose I characteristics. These feedstock differences were considered in relation to their dissolution behavior in aqueous NaOH.

Dissolution proceeded through swelling and mercerization; however, complete dissolution was not achieved for either cellulose sample under the conditions examined. BC consistently showed lower solubility than CC. This difference may be related to the longer particle length and higher *DPv* of BC, which can limit solvent penetration and the transfer of cellulose chains into the alkali-dissolved fraction under the present conditions.

The *DPv* values of the recovered cellulose products were lower than those of the starting materials and converged to approximately 180. This convergence was interpreted as an apparent *DPv* limitation of the recovered cellulose fraction, rather than as direct evidence of selective dissolution. Particle-length fractionation of BC increased the fraction of shorter particles, decreased *DPv*, and improved solubility, indicating that feedstock fractionation is a practical approach for improving the dissolution behavior of BC in this aqueous NaOH system.

As a proof-of-concept recovery experiment, alkali-dissolved BC and CC fractions were recovered using aqueous acetic acid. The recovered products showed structural features consistent with cellulose II formation. However, the recovered specimens were brittle and structurally heterogeneous under the present non-optimized conditions; therefore, the recovery process should be regarded as a preliminary demonstration of cellulose recovery rather than optimized fiber production.

Overall, this study clarifies practical feedstock-related factors associated with the dissolution of bamboo-derived cellulose in low-temperature aqueous NaOH, particularly particle length and *DPv*. The results provide useful guidance for improving the processing of bamboo-derived cellulose powders and for developing simple recovery routes for cellulose products using aqueous acid treatment.

ACKNOWLEDGEMENTS: The authors thank Oita CELEENA Co. Ltd. for supplying the BC. This study was partially supported by the Oita University President's Strategic Discretionary Fund.

REFERENCES

[1] K. Kamide, K. Okajima, T. Matsui and K. Kowsaka, *Polymer J.*, **24**, 71 (1992), https://doi.org/10.1295/polymj.24.71

[2] S. Yamane, T. Aoyagi, M. Ago, K. Sato, K. Okajima *et al.*, *Sen-i Gakkaishi*, **52**, 310 (1996), https://doi.org/10.2115/fiber.52.6_310

[3] A. Isogai and R. H. Atalla, *Cellulose*, **5**, 309 (1998), https://doi.org/10.1023/A:1009272632367
[4] R. Sescousse and T. Budtova, *Cellulose*, **16**, 417 (2009), https://doi.org/10.1007/s10570-009-9287-z
[5] R. Li, S. Wang, A. Lu and L. Zhang, *Cellulose*, **22**, 339 (2015), https://doi.org/10.1007/s10570-014-0542-6
[6] B. Swensson, A. Idström, A. Larsson and M. Hasani, *Cellulose*, **27**, 101 (2020), https://doi.org/10.1007/s10570-019-02780-8
[7] U. Chaudhary, S. Malik, V. Rana and G. Joshi, *Adv. Bamboo Sci.*, **7**, 100069 (2024), https://doi.org/10.1016/j.bamboo.2024.100069
[8] T. Tsuboi, S. Yokota, S. Tagawa and T. Kondo, *Nord. Pulp Pap. Res. J.*, **29**, 69 (2014), https://doi.org/10.3183/npprj-2014-29-01-p069-076
[9] K. Yamashiro and H. Nishida, *Int. J. Biomass Renew.*, **4**, 8 (2015), https://kyutech.repo.nii.ac.jp/record/4413/files/49_111_pmoaz15-12-29.pdf
[10] M. Guimarães, V. R. Botaro, K. M. Novack, W. P. Flauzino Neto, L. M. Mendes *et al*., *J. Nanosci. Nanotechnol.*, **15**, 6751 (2015), https://doi.org/10.1166/jnn.2015.10854
[11] The Japanese Pharmacopoeia. Specifications and Tests for Pharmaceutical Excipients and Products, Ministry of Health, Labour and Welfare, Tokyo, Japan, 18th ed., 2025, 51-0803-0, 51-0802-0. https://www.mhlw.go.jp/content/11121000/001329453.pdf (accessed 16 January 2026)
[12] Y. Shimosako, E. Miyazaki, Y. Masuda, K. Tojo, M. Matsuoka *et al*., *CEAS Space J.*, **56**, e00205 (2026), https://doi.org/10.1007/s12567-025-00692-x
[13] A. Isogai and M. Usuda, *Sen-i Gakkaishi*, **45**, 324 (1989), https://doi.org/10.2115/fiber.46.8_324
[14] W. Xu, M. A. Khan, A. Ullah, A. He, Z. Wu *et al*., *Int. J. Biol. Macromol.*, **246**, 125649 (2023), https://doi.org/10.1016/j.ijbiomac.2023.125649
[15] J. Zhou and L. Zhang, *Polym. J.*, **32**, 866 (2000), https://doi.org/10.1295/polymj.32.866
[16] Y. Kojima, M. Takayasu, M. Tama and S. Koda, *Ultrason. Sonochem.*, **51**, 419 (2018), https://doi.org/10.1016/j.ultsonch.2018.07.030